

# PP2A phosphatase is required for dendrite pruning via actin regulation in *Drosophila*

Neele Wolterhoff, Ulrike Gigengack & Sebastian Rumpf\* 

## Abstract

**Large-scale pruning, the developmentally regulated degeneration of axons or dendrites, is an important specificity mechanism during neuronal circuit formation. The peripheral sensory class IV dendritic arborization (c4da) neurons of *Drosophila* larvae specifically prune their dendrites at the onset of metamorphosis in an ecdysone-dependent manner. Dendrite pruning requires local cytoskeleton remodeling, and the actin-severing enzyme Mical is an important ecdysone target. In a screen for pruning factors, we identified the protein phosphatase 2 A (PP2A). PP2A interacts genetically with the actin-severing enzymes Mical and cofilin as well as other actin regulators during pruning. Moreover, *Drosophila* cofilin undergoes a change in localization at the onset of metamorphosis indicative of a change in actin dynamics. This change is abolished both upon loss of Mical and PP2A. We conclude that PP2A regulates actin dynamics during dendrite pruning.**

**Keywords** actin; dendrite; phosphatase; PP2A; pruning

**Subject Categories** Cell Adhesion, Polarity & Cytoskeleton; Neuroscience; Post-translational Modifications & Proteolysis

**DOI** 10.15252/embr.201948870 | Received 15 July 2019 | Revised 27 February 2020 | Accepted 4 March 2020 | Published online 24 March 2020

**EMBO Reports (2020) 21: e48870**

## Introduction

Neurite pruning, the physiological degeneration of axons or dendrites during development, is an important specificity mechanism during neuronal circuit formation [1,2]. While the mechanisms of neurite outgrowth and synapse formation have been studied in some detail, comparably little is known about the mechanisms underlying pruning. In holometabolous insects, pruning occurs at large scale during metamorphosis to remove larval-specific neurites. In the peripheral nervous system (PNS) of *Drosophila*, the so-called class IV dendritic arborization (c4da) neurons specifically prune their long and branched larval dendrites at the onset of the pupal phase by a degenerative mechanism [3,4]. C4da neuron dendrite pruning is induced by a prepupal peak in the steroid hormone ecdysone [3,4]. Ecdysone acts cell-autonomously in c4da neurons by inducing the expression of pruning genes such as the transcription

factor Sox14 and the actin-severing enzyme Mical [5], an oxidoreductase that can sever actin filaments through actin oxidation [6], as well as the putative growth regulator headcase [7]. The first morphological signs of dendrite pruning are seen at around 3–5 h after puparium formation (h APF), when dendrites start to show local thinnings and varicosities in their proximal regions that appear to be due to changes in cytoskeletal and membrane stability. At these proximal sites, the dendrites are eventually severed between 6 and 12 h APF. Known pathways that contribute to this destabilization of the proximal dendrites are local microtubule disassembly [4,8,9] and alterations in plasma membrane trafficking [10–13]. Microtubule disassembly is induced by a signal transduction cascade involving the kinase Par-1 which negatively regulates the microtubule-associated protein tau to enhance microtubule dynamics [9]. Loss of microtubules starts at proximal dendrite branch-points and proceeds with a proximal-to-distal directionality [14]. Dendritic microtubules display a uniform plus end-in orientation, and this uniformity is required for dendrite pruning [14]. Together with the observed directionality of microtubule breakdown, this indicates that microtubule breakdown occurs mostly from plus ends during dendrite pruning and that microtubule polarity acts as a spatial determinant [15]. Once severed, pruned dendrites are subsequently fragmented in a caspase-dependent manner and phagocytosed by epidermal cells [16,17].

While the roles and importance of microtubule regulation during pruning are emerging, relatively little is known about actin regulation during the process. While it is clear that the actin-severing enzyme Mical is induced in c4da neurons at the onset of the pupal stage and is required for dendrite pruning [5], it is not known whether it affects actin structures at this stage, and whether other actin regulators are involved in dendrite pruning. This is somewhat surprising because actin dynamics play important roles during earlier larval c4da neuron dendrite development. For example, Arp2/3-dependent actin polymerization promotes dendrite branching [18], and this also requires the actin disassembly factor cofilin to increase actin dynamics [19]. One factor that has recently been implicated in actin regulation during larval c4da neuron dendrite development is Widerborst (Wdb), encoding a regulatory B subunit of protein phosphatase 2A (PP2A) [20]. PP2A is known to regulate both microtubules, e.g., through tau [21], and actin, e.g., through Rho GTPases or regulators of cortical actin [22,23]. It is a trimeric protein complex consisting of an A subunit that acts as a scaffold

(encoded by PP2A-29B in flies), a C subunit containing the active site (encoded by *microtubule star/mts*), and one of several regulatory B subunits. In addition to Wdb, the B subunit Twins (Tws) has also been linked to actin regulation during imaginal disk development [24].

In this study, we identify PP2A as a regulator of c4da neuron dendrite pruning. In a survey of phosphoregulators of dendrite pruning, we found that loss of the scaffold subunit PP2A-29B caused strong dendrite pruning defects. The catalytic subunit mts and—in a somewhat redundant manner, the B subunits Wdb and Tws are also required for this process, indicating the involvement of a specific PP2A holoenzyme. During dendrite pruning, PP2A displays genetic interactions with Mical, the actin disassembly factor cofilin and other actin regulators, indicating that PP2A acts via regulated actin disassembly during the process.

## Results

### The serine/threonine phosphatase PP2A is required for c4da neuron dendrite pruning

In order to identify phosphoregulators of c4da neuron dendrite pruning, we expressed dsRNA constructs targeting signaling molecules under the control of the c4da neuron-specific GAL4 driver *ppk-GAL4* and visualized c4da neurons by coexpression of membrane-bound GFP. Control c4da neurons expressing *Orco* dsRNA (against *Odorant receptor co-receptor* which is not expressed in c4da neurons) have long and branched dendrites at the third-instar larval stage (Fig 1A), which are completely and specifically pruned at 18 h APF (Fig 1A', G, and H). Loss of *PP2A-29B*, encoding the A subunit of the serine/threonine phosphatase PP2A, or the catalytic C subunit encoded by *Microtubule star (mts)*, caused a decrease in branching and dendritic field coverage at the third-instar larval stage (Figs 1B–F and EV1). At 18 h APF, *PP2A-29B* knock-down caused dendrite pruning defects (Fig 1B'). This phenotype was highly penetrant, as most c4da neurons showed pruning defects at this stage (Fig 1G), and also very severe, as most neurons retained many primary and secondary dendrites still attached to the soma (Fig 1H). In order to confirm this result, we next used Mosaic Analysis with a Repressible Cell Marker (MARCM) [25] to generate homozygous *PP2A-29B* mutant c4da neurons. C4da neurons homozygous for the loss-of-function allele *PP2A-29B<sup>GE16781</sup>* also displayed dendrite pruning defects at 18 h APF (Fig 1C', G, and H). Furthermore, these pruning defects could be rescued by GAL4/UAS-mediated expression of HA-tagged *PP2A-29B* in the MARCM clones (Fig 1D', G, and H).

In order to assess the requirement for PP2A catalytic activity, we next expressed a dominant-negative version of the catalytic subunit, dnMts, in c4da neurons. Similar to the effects of *PP2A-29B* downregulation, the expression of dnMts caused strong and penetrant dendrite pruning defects at 18 h APF (Fig 1E, E', G, and H). In order to confirm this result, we again used MARCM to create c4da neurons homozygous for *mts<sup>s5286</sup>*, a P element insertion in the *Mts* gene. These c4da neurons also displayed strong dendrite pruning defects (Fig 1F–H).

In order to test which B subunit might be involved in the regulation of c4da neuron dendrite pruning, we used sgRNAs or dsRNA

constructs for tissue-specific CRISPR and/or RNAi, as well as mutant analyses. The four B/B' subunits in the fly genome are encoded by *Twins* (Tws), *PR72/CG4733*, *Well rounded* (Wrd), and *Widerborst* (Wdb). While the expression of an sgRNA construct directed against CG4733 under *ppk-GAL4* did not cause dendrite pruning defects at 18 h APF, an sgRNA construct against *Tws* resulted in mild pruning defects (Fig EV2A–D). The expression of a dsRNA construct against Wrd did not cause significant dendrite pruning defects (Fig EV2F), while the expression of a dsRNA construct against Tws again caused very mild defects (Fig EV2G and J). In order to manipulate *Widerborst*, we used the mutant allele *wdb<sup>14</sup>* for MARCM analysis. Homozygous *wdb<sup>14</sup>* c4da neuron MARCM clones displayed clear dendrite pruning defects (Fig EV2H). However, the penetrance of these defects was still lower than expected from the very strong defects caused by manipulation of *PP2A-29B* or *Mts*. PP2A B subunits can sometimes act in a redundant manner [26]. To address this possibility, we expressed Tws dsRNA in c4da neurons in a *wdb<sup>14</sup>/+* heterozygous mutant background. This manipulation caused stronger dendrite pruning defects more similar to those caused by loss of *PP2A-29B* or *Mts* (Fig EV2I and J), indicating that these two B subunits can regulate pruning redundantly. Taken together, our data indicate that a PP2A holoenzyme complex is required for c4da neuron dendrite pruning.

### PP2A does not interact with the Par-1/tau microtubule pathway during dendrite pruning

We next asked how PP2A could regulate dendrite pruning. Because the role of PP2A in cytoskeleton regulation is well established, we wanted to assess a potential role for PP2A in microtubule disassembly. To this end, we expressed *PP2A-29B* dsRNA in c4da neurons and tested whether upregulation of the microtubule disassembly pathway(s) involved in dendrite pruning could ameliorate the dendrite pruning defects caused by this treatment. *Tau* heterozygosity or overexpression of Par-1 or kat-60L1 did not cause dendrite pruning defects by themselves (Fig EV3A–E). We next assessed whether these manipulations suppressed the pruning defects induced by *PP2A* downregulation. In order to control for potential UAS titration effects, we compared the effects of *PAR-1* and *kat-60L1* overexpression to overexpression of *lacZ*. However, none of the microtubule manipulations suppressed the pruning defects induced by loss of *PP2A-29B* (Fig EV3F–J), suggesting that the function of PP2A during c4da neuron dendrite pruning is not linked to Par-1/tau-mediated microtubule regulation.

The pruning defects caused by loss of PP2A also seemed qualitatively different from the defects caused by loss of PAR-1. Pruning dendrites of control c4da neurons develop varicosities as a sign of degeneration during the early pruning stages between approximately 3 h APF and 12 h APF [10]. These varicosities are round, occur in thinned regions of (proximal) dendrites, and are usually smaller than 5  $\mu$ m in diameter. In contrast, unpruned c4da neuron dendrites expressing *PP2A-29B* dsRNA displayed varicosities at 18 h APF that were larger and often occurred at distal dendrite tips. Sometimes, they developed small filopodia-like protrusions (e.g., Fig EV4C), somewhat reminiscent of axonal growth cones, and these varicosities also were positive for the actin marker lifeact::GFP [27]. In unpruned dendrites of c4da neurons lacking PAR-1, only small, proximal varicosities could be seen that were reminiscent of

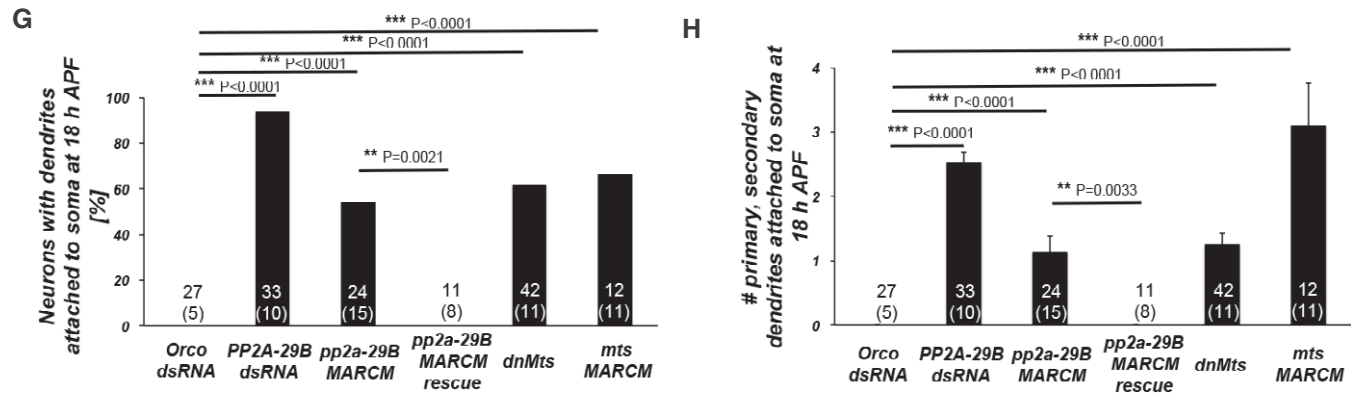
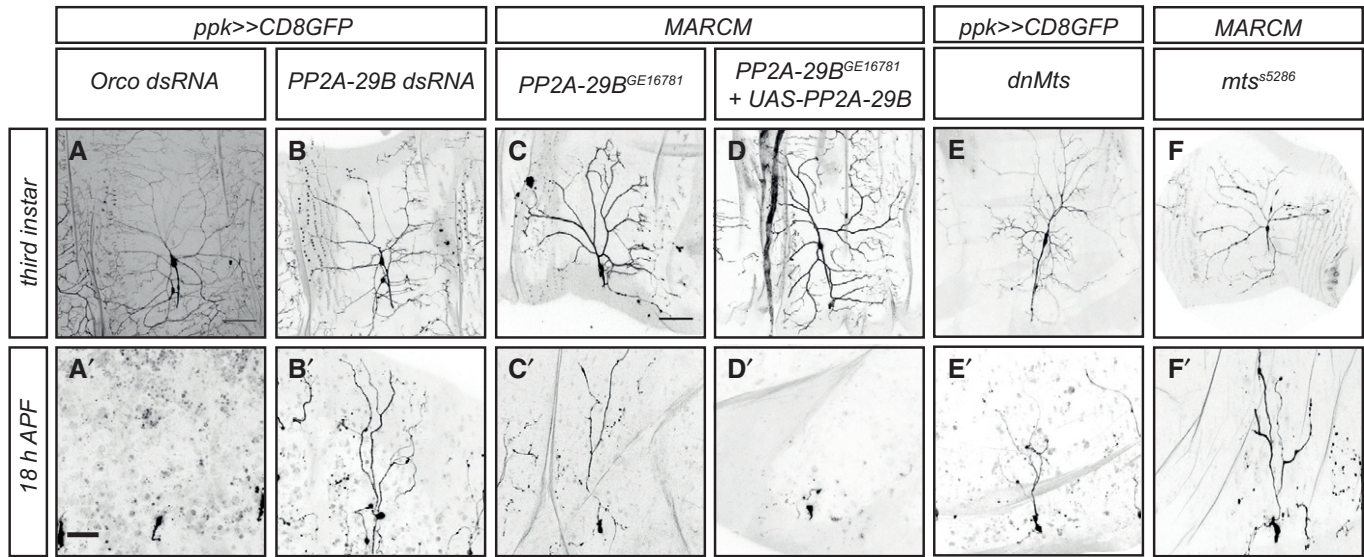


**Figure 1. PP2A is required for dendrite pruning.**

A–F' Upper panels (A–F) show morphology of c4da neurons of the indicated genotypes at the third-instar larval stage, and lower panels (A'–F') show c4da neuron morphology at 18 h after puparium formation (APF). Neurons were labeled by CD8::GFP expression under *ppk-GAL4* or by tdTomato expression in MARCM clones. (A, A') C4da neurons expressing control Orco dsRNA. Scale bars are 100  $\mu$ m in (A) (for larval images) and 50  $\mu$ m in (A') (for pupal images). (B, B') C4da neurons expressing PP2A-29B dsRNA. (C, C') Homozygous *PP2A-29B<sup>GE16781</sup>* mutant c4da neuron MARCM clones. (D, D') Homozygous *PP2A-29B<sup>GE16781</sup>* mutant c4da neuron MARCM clones expressing UAS-<sup>HA</sup>PP2A-29B. (E, E') C4da neurons expressing dominant-negative Mts. (F, F') Homozygous *mts<sup>s5286</sup>* mutant c4da neuron MARCM clones.

G Penetrance of pruning defects at 18 h APF in (A'–E'). \*\**P* < 0.005, \*\*\**P* < 0.0005, Fisher's exact test. The number of neurons for each genotype is given in the figure, and the number of animals is given below in parentheses.

H Severity of pruning defects at 18 h APF in (A'–E') as assessed by number of primary and secondary dendrites attached to soma at 18 h APF. Data are mean  $\pm$  s.d., \*\**P* < 0.005, \*\*\**P* < 0.0005, Wilcoxon's test. Numbers of neurons (animals) for each genotype are given in the figure.

the ones normally occurring in earlier (Fig EV4A–D, arrow in Fig EV4B).

### PP2A interacts genetically with ecdysone target genes

During c4da neuron dendrite pruning, the steroid hormone ecdysone induces the expression of important pruning genes, in particular the transcription factor Sox14 and the actin-severing enzyme Mical. We therefore tested next whether Sox14 or Mical might interact with PP2A during dendrite pruning. Overexpression of *Sox14* or *Mical* alone did not cause dendrite pruning defects (Fig 2A–C). However, *Sox14* overexpression significantly reduced the severity of

the dendrite pruning defects induced by loss of *PP2A-29B*, as assessed by the reduced number of dendrites attached to the soma under these conditions (Fig 2F, G, K, and L). Mical overexpression caused a significant reduction in both penetrance and severity of the pruning defects caused by *PP2A-29B* knockdown (Fig 2H, K, and L). In order to address whether actin-related domains of Mical, such as the oxidoreductase domain and the calponin homology (CH) domain, a putative actin binding site [28], are required for this genetic interaction, we next tested whether the expression of Mical mutants lacking these domains could also suppress the dendrite pruning defects induced by *PP2A-29B* knockdown. Overexpression of *MicalAredox* alone in *c4da* neurons did not cause dendrite

pruning defects (Fig 2D, K, and L) but failed to suppress the effects of PP2A-29B dsRNA (Fig 2I, K, and L). Interestingly, overexpression of *Mical**ACH* in c4da neurons alone had a dominant effect and caused strong dendrite pruning defects (Fig 2E, K, and L), possibly reflecting a direct involvement of this domain in the catalytic cycle of Mical. Consistently, coexpression of *Mical**ACH* with *PP2A-29B* dsRNA strongly enhanced the severity of the dendrite pruning defects (Fig 2J–L). While Mical overexpression strongly suppressed the pruning defects caused by loss of PP2A, it did not significantly affect the larval dendrite defects (Fig EV1), suggesting that the mechanistic basis underlying these defects may not be identical. Taken together, these data indicate that the role of PP2A during dendrite pruning is linked to the ecdysone targets *Sox14* and *Mical*, and the actin-modifying domains of Mical are crucial for this.

### Effects of PP2A on Sox14 and Mical expression

*Sox14* and *Mical* are both transcriptionally induced by the ecdysone receptor at the onset of the pupal stage [5]. The observed genetic interactions between PP2A and these two factors could therefore reflect a defect in *Sox14* and/or *Mical* expression (and hence a defect in ecdysone-mediated gene expression). To address this possibility, we next assessed the effects of PP2A knockdown on *Sox14* and *Mical* expression by immunofluorescence. At 2 h APF, *Sox14* can be detected in the nucleus of control c4da neurons (Fig 3A). In order to downregulate PP2A, we next expressed either *PP2A-29B* dsRNA or dominant-negative Mts in c4da neurons and assessed the effects on *Sox14* expression. While *PP2A-29B* knockdown did not affect *Sox14* expression (Fig 3B and D), *Sox14* levels seemed to be increased upon dnMts expression (Fig 3C and D).

At 2 h APF, *Mical* is also robustly expressed in c4da neurons and localizes to the cytoplasm (Fig 3E). *Mical* was also normally expressed in neurons expressing *PP2A-29B* dsRNA (Fig 3F and J). Surprisingly, many c4da neurons expressing dnMts showed strongly reduced *Mical* staining at this stage (Fig 3G and J). To address these potentially contradictory results, we reassessed *Mical* expression at the white pupal stage (0 h APF). At this stage, c4da neurons expressing *PP2A-29B* dsRNA also displayed reduced *Mical* levels (Fig 3H–J). We interpret these data as indicating a 2-h delay in *Mical* expression upon PP2A downregulation. However, dendrite severing and pruning take place between 5 h APF and 10 h APF. We assess pruning phenotypes at 18 h APF, and the pruning defects induced by *PP2A-29B* knockdown are still highly penetrant and severe at this much later stage. We therefore conclude that the observed genetic interactions between PP2A and *Sox14*/*Mical* cannot be explained through a role of PP2A in *Mical* gene expression alone.

### PP2A-linked pruning defects can be suppressed by cofilin overexpression

The observation that PP2A interacts with *Mical* during dendrite pruning prompted us to investigate whether PP2A could be linked to actin regulation during this process. We therefore asked whether upregulation of a different actin-severing activity could also suppress the pruning defects caused by loss of PP2A. Cofilin is a well-characterized actin depolymerization factor that can also functionally cooperate with *Mical* [29]. We first asked whether

*Drosophila* cofilin, encoded by *Twinstar* (*tsr*), was itself required for c4da neuron dendrite pruning. MARCM clones homozygous for the cofilin mutant allele *tsr*<sup>N121</sup> did not display dendrite pruning defects at 18 h APF (Fig EV5A). However, *tsr* overexpression caused a partial suppression of the pruning defects upon *PP2A-29B* knockdown compared to the *lacZ* titration control (Fig 4A, D, E, H, and I).

Cofilin is inhibited by phosphorylation by LIM kinase [30,31] and activated through dephosphorylation by slingshot phosphatases [32], and this is important for neuronal morphogenesis [33]. Consequently, nonphosphorylatable versions of *tsr* are constitutively active, and phosphomimetic *tsr* mutant versions are inactive. Overexpression of UAS transgenes encoding nonphosphorylatable *tsr*<sup>S3A</sup> or phosphomimetic *tsr*<sup>S3E</sup> alone did not cause dendrite pruning defects (Fig 4B and C). UAS-*tsr*<sup>S3A</sup> afforded a similar, but not better, suppression of the pruning defects induced by PP2A knockdown as UAS-*tsr* *wt* (Fig 4F, H, and I), indicating that the phosphorylation state of cofilin does not affect its ability to suppress PP2A. UAS-*tsr*<sup>S3E</sup> enhanced the severity of the pruning defects upon PP2A knockdown, consistent with a mild dominant or synergistic effect (Fig 4G–I).

We also wished to assess the localization of cofilin in c4da neurons. To this end, we used transgenic N-terminally GFP-tagged *Drosophila* *tsr* driven by the GAL4/UAS system (UAS-GFP::*tsr*). GFP::*tsr* localized to multiple punctate, sometimes elongated structures in the soma and dendrites of c4da neurons during the larval stage (Figs 4J and M, and EV5). These GFP::*tsr* punctae were reminiscent of cofilin/actin aggregates that can be induced by cofilin overexpression or stress in mammalian cells [34]. In support of the idea that these punctae contained actin, GFP::*tsr* also strongly localized to the dendritic “spikes” on the dendrites of c3da neurons that are known to be actin-rich [35] (Fig EV5D) (the *ppk-GAL4* insertion used for GFP::*tsr* expression in these experiments is also stochastically expressed in c3da neurons). At 6 h APF, most GFP::*tsr* punctae in c4da neurons had vanished and GFP::*tsr* now displayed a largely dispersed distribution (Fig 4J' and M). Notably, one or two bright elongated GFP::*tsr* accumulations could still be seen at this stage that localized proximally to dendritic thinnings in primary dendrites (Fig 4J'). This localization was somewhat reminiscent of the localization of active cofilin in filopodia [36]. C4da neurons expressing *Mical* dsRNA had a similar number of GFP::*tsr* punctae as control neurons at the larval stage (Fig 4K and M). However, several c4da neurons expressing *Mical* dsRNA still displayed many GFP::*tsr* accumulations at 6 h APF (Fig 4K' and M), indicating that *Mical* was required for the observed changes in GFP::*tsr* localization between larvae and pupae. In contrast to control neurons, GFP::*tsr* was evenly dispersed in larval c4da neurons expressing *PP2A-29B* dsRNA, with no punctae visible (Fig 4L and M). At 6 h APF, such GFP::*tsr* accumulations were also not seen at the bases of proximal dendrites in these neurons (Fig 4L' and M). Thus, PP2A interacts genetically with actin disassembly factors and affects the localization of cofilin in c4da neurons.

### Loss of PP2A can be ameliorated by manipulation of actin regulators

In order to deepen the links between PP2A and actin regulation during dendrite pruning, we next sought to identify additional genetic interactions between PP2A and actin. To this end, we

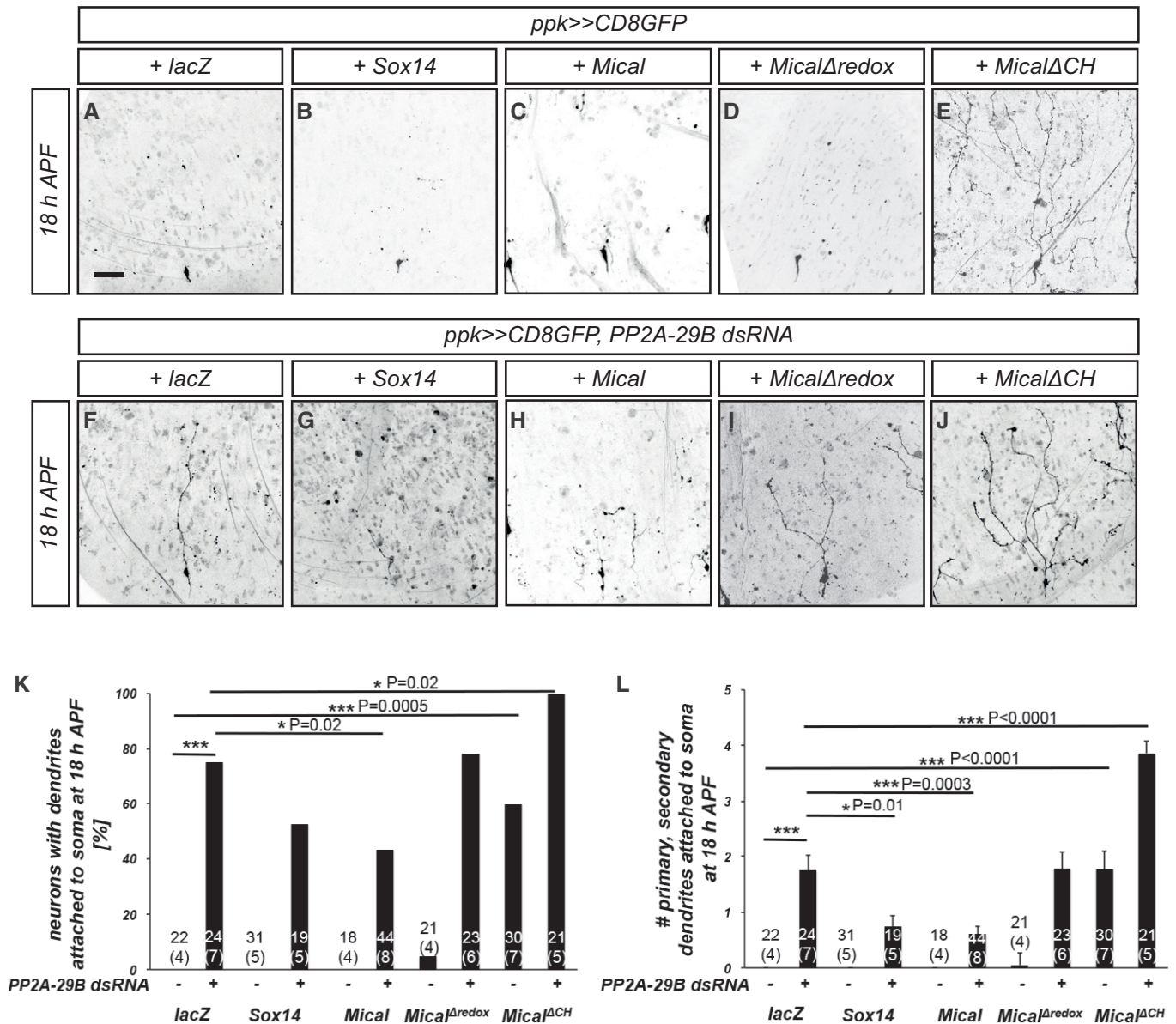


**Figure 2. PP2A interacts genetically with the Sox14/Mical pathway.**

A–J) The indicated Sox14 or Mical constructs were tested for their ability to suppress pruning defects induced by PP2A-29B dsRNA expression. C4da neurons were labeled by CD8::GFP expression under *ppk-GAL4*, and dendrite pruning defects were assessed at 18 h APF. Panels (A–E) show effects of Sox14/Mical pathway manipulations alone, and panels (F–J) show neurons coexpressing PP2A-29B dsRNA. The scale bar in (A) is 50  $\mu$ m. (A, F) C4da neurons (co-)expressing lacZ. (B, G) C4da neurons (co-)expressing Sox14. (C, H) C4da neurons (co-)overexpressing Mical. (D, I) C4da neurons (co-)expressing Mical $\Delta$ redox. (E, J) C4da neurons (co-)expressing Mical $\Delta$ CH.

K) Penetrance of pruning defects in panels (A–J). \**P* < 0.05, \*\*\**P* < 0.0005, Fisher’s exact test. Numbers of neurons (animals) for each genotype are given in the figure, and the numbers of animals are given below in parentheses.

L) Severity of pruning defects in panels (A–J) as assessed by number of primary and secondary dendrites attached to soma at 18 h APF. Data are mean  $\pm$  s.d., \**P* < 0.05, \*\*\**P* < 0.0005, Wilcoxon’s test. Numbers of neurons (animals) for each genotype are given in the figure.

downregulated known actin regulators and asked whether this could ameliorate the pruning defects caused by loss of PP2A. As a control, we expressed GFP::tsr in this background. While GFP::tsr did not reduce the penetrance of the pruning defects induced by PP2A-29 dsRNA, when compared to overexpression of tdTomato, it decreased their severity (Fig 5A, B, I, and J). This suppression was lower than with untagged tsr, but this could be due to lower

expression levels of GFP::tsr (this construct is a site-directed transgene which in our experience has lower expression when compared to randomly inserted ones). Rac family GTPases are another prominent class of actin regulators. While inhibition of Rac1 with a dominant-negative construct did not ameliorate the dendrite pruning defects induced by PP2A-29 dsRNA, inhibition of Rho with a dominant-negative construct reduced the severity of the pruning defects

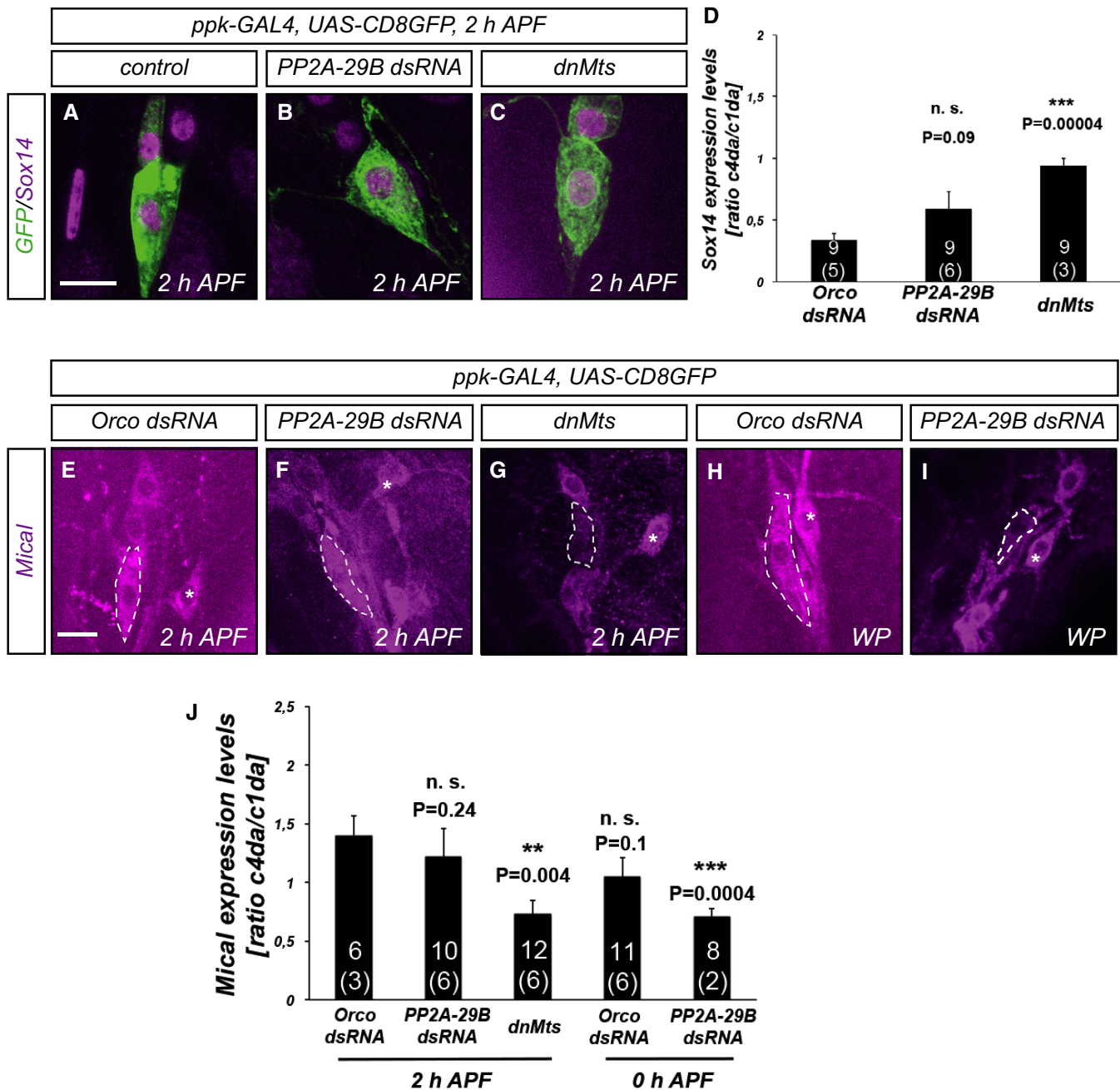


**Figure 3. Effects of PP2A on ecdysone target gene expression during dendrite pruning.**

C4da neurons were labeled by CD8::GFP expression under *ppk-GAL4*, and the expression of Sox14 or Mical was assessed by immunofluorescence.

A–C Sox14 stainings at 2 h APF. (A) Control c4da neurons. (B) C4da neurons expressing PP2A-29B dsRNA. (C) C4da neuron expressing dominant-negative Mts.

D Quantification of Sox14 expression in (A–C). C4da neuron Sox14 expression was normalized to Sox14 expression in neighboring ddaE c1da neurons (identified by characteristic cell body shape). Data are mean  $\pm$  s.d. The numbers of neurons (animals) for each genotype are given in each graph (data were not derived from independent experiments). n.s., not significant, \*\*\* $P < 0.0005$ , Wilcoxon's test.

E–I Mical stainings at the indicated time points. (E) Mical expression in control c4da neurons at 2 h APF. (F) Mical expression in c4da neurons expressing dominant-negative Mts at 2 h APF. (G) Mical expression in c4da neurons expressing PP2A-29B dsRNA at 2 h APF. (H) Mical expression in c4da neurons expressing Orco dsRNA at the white pupal (WP) stage (0 h APF). (I) Mical expression in c4da neurons expressing PP2A-29B dsRNA at the white pupal stage (0 h APF).

J Quantification of Mical expression in (E–I). C4da neuron Mical expression was normalized to Mical expression in neighboring ddaE c1da neurons (marked by asterisks). Data are mean  $\pm$  s.d. The numbers of neurons (animals) for each genotype are given in each graph (data were not derived from independent experiments). n.s., not significant, \*\* $P < 0.005$ , \*\*\* $P < 0.0005$ , Wilcoxon's test.

Data information: Scale bars in (A and E) are 10  $\mu$ m.

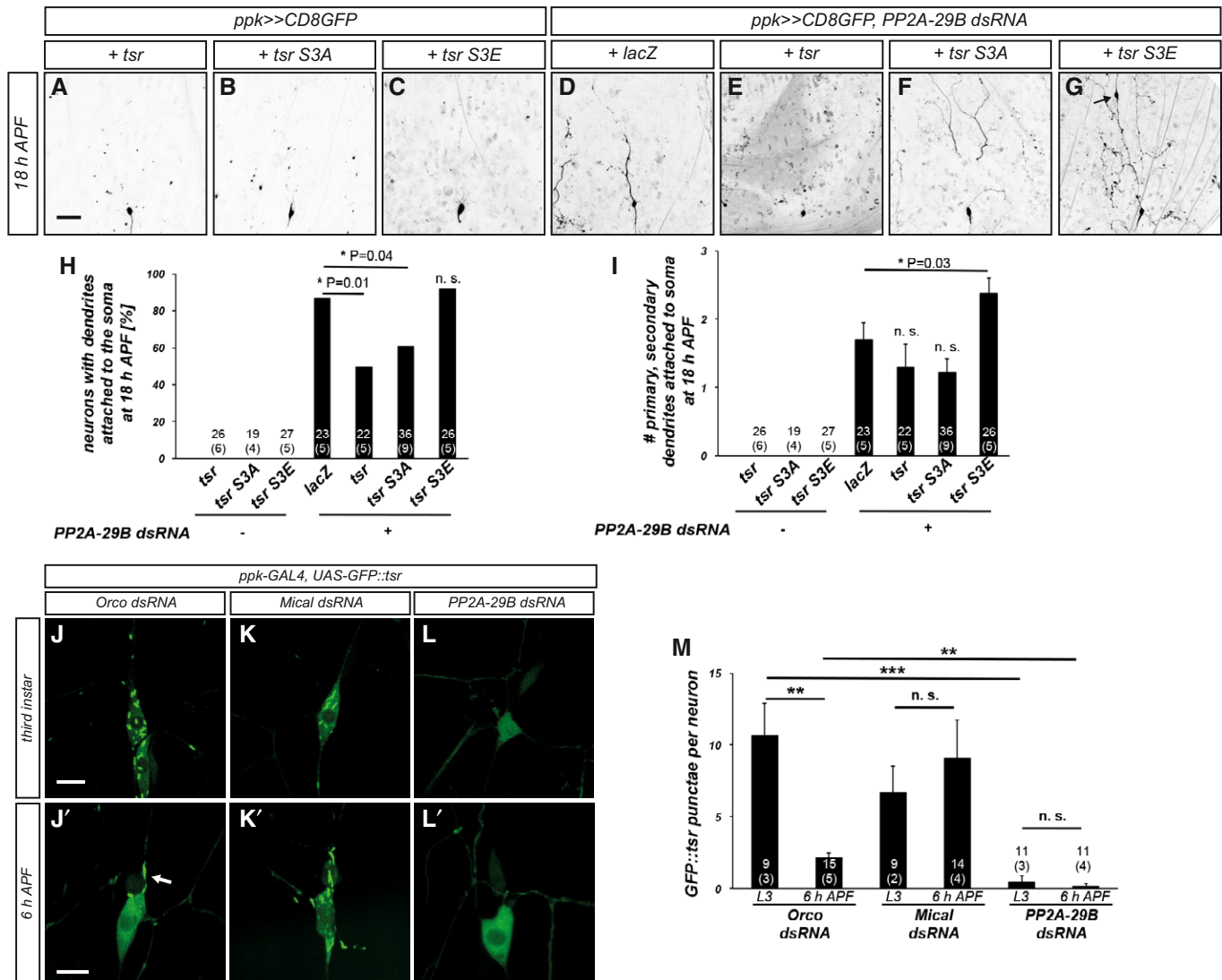


**Figure 4. Interactions between PP2A and the actin regulator cofilin during c4da neuron dendrite pruning.**

A–G The indicated UAS-*tsr* constructs were tested for their ability to suppress pruning defects induced by PP2A-29B dsRNA expression. Suppression tests were performed as in Fig 2. Panels (A–C) show effects of the expression of wild-type or phosphomutant *tsr* variants on dendrite pruning, and panels (D–G) show neurons coexpressing PP2A-29B dsRNA. (A, E) C4da neuron (co-)overexpressing wild-type *tsr*. (B, F) C4da neuron (co-)overexpressing *tsr* S3A. (C, G) C4da neuron (co-)overexpressing *tsr* S3E. The arrow in panel G denotes a characteristic varicosity at the tip of an unpruned dendrite. (D) C4da neuron coexpressing PP2A-29B dsRNA and *lacZ* as a UAS titration control.

H Penetrance of pruning defects in panels (A–C). \**P* < 0.05, Fisher's exact test. Numbers of neurons (animals) for each genotype are given in the figure.

I Severity of pruning defects in panels (A–C) as assessed by number of primary and secondary dendrites attached to soma at 18 h APF. Data are mean ± s.d., \**P* < 0.05, Wilcoxon's test. Numbers of neurons (animals) for each genotype are given in the figure.

J–L GFP-tagged *Drosophila* cofilin (GFP::tsr) was expressed in c4da neurons under *ppk-GAL4*, and its localization was assessed at the indicated developmental stages by live imaging. Panels (J–L) show GFP::tsr localization in c4da neurons at the third-instar stage, and panels (J'–L') show GFP::tsr localization in c4da neurons at 6 h APF. (J, J') Control c4da neurons expressing Orco dsRNA. (K, K') C4da neurons expressing Mical dsRNA. (L, L') C4da neurons expressing PP2A-29B dsRNA.

M Quantification of GFP::tsr punctae in samples (J–L). Data are mean ± s.d., and the numbers of neurons (animals) analyzed for each genotype are given in the figure (data were not derived from independent experiments). \*\**P* < 0.005, \*\*\**P* < 0.0005, n.s., not significant, Wilcoxon's test.

Data information: Scale bars are 50 μm in (A) and 10 μm in (J).

significantly, such that each neuron had fewer dendrite branches attached to the soma at 18 h APF (Fig 5C, D, I, and J). In order to manipulate additional regulators of actin polymerization, we next used mutants or dsRNA constructs. Partial loss of the actin polymerase *enabled* in a heterozygous *ena*<sup>210/+</sup> mutant background did not have an effect on the severity of the pruning defects (Fig 5E, I,

and J). Downregulation of profilin, an actin binding protein involved in the regulation of actin dynamics, significantly reduced the effects of PP2A-29B dsRNA when compared to an Orco control dsRNA (Fig 5F, G, I, and J). The strongest suppression of the severity of the pruning defects was achieved by downregulation of the cortical actin regulator moesin (Fig 5H–J).

We also performed an overexpression survey to identify possible kinases counteracting PP2A. While overexpression of LIM kinase, active atypical protein kinase C (aPKC), or abelson kinase (*abl*, a tyrosine kinase), did not cause dendrite pruning defects, overexpression of a constitutively active form of protein kinase A (PKA *mc\**) caused strong and fully penetrant *c4da* neuron dendrite pruning defects (Fig EV6). However, neither inhibition of PKA nor the previously identified negative pruning regulator TOR [37] could suppress the pruning defects caused by PP2A knockdown (Fig EV6).

Taken together, our results suggest that PP2A regulates one or several aspects of actin dynamics and/or cortical actin organization that are required for dendrite pruning.

## Discussion

In this study, we identified an important role for the protein phosphatase PP2A during large-scale dendrite pruning of *Drosophila* *c4da* neurons during metamorphosis. Our data indicate that a PP2A holoenzyme containing either the *Wdb* or *Tws* regulatory subunit is involved in pruning regulation. Our data strongly link PP2A to actin regulation during dendrite pruning. In particular, our genetic interaction studies show that the pruning defects caused by loss of PP2A can be suppressed by overexpression of the actin-severing enzyme Mical. Mical is induced by ecdysone at the onset of the pupal stage and is required for *c4da* neuron dendrite pruning. While our data and an accompanying study by Yu and colleagues [38] show that induction of Mical expression is delayed by loss of PP2A, this effect is transient, and there is no strong effect on Mical expression at 2 h APF, when other mutants that directly affect Mical expression still show strongly reduced Mical levels (e.g., Ref. [39,40]). While the delay in Mical expression could contribute to the observed pruning defects, several lines of evidence indicate that PP2A has an additional function in actin regulation, such as the observations that the actin-related domains of Mical are required for suppression of the PP2A phenotype (Fig 2) and that overexpression of cofilin can also partially rescue the PP2A phenotype (Fig 4). Furthermore, our genetic analyses (Fig 5) link PP2A to actin dynamics and cortical actin organization. In this context, it is interesting that *c4da* neurons lacking PP2A had an altered distribution of GFP::*tsr* (GFP-tagged cofilin) (Fig 4). This transgene localized to punctate structures upon GAL4-mediated expression. It is known that active cofilin can co-assemble with actin into so-called cofilin rods that resemble actin/cofilin structures at the base of filopodia where actin turnover is high [36]. As GFP::*tsr* also localizes to the actin-rich dendritic spikes of *c3da* neurons (Fig EV5), it is interesting to speculate that the formation of these structures may in part reflect the overall F-actin amount in the cell, or a cell's propensity to form F-actin. The lack of GFP::*tsr* punctae in *c4da* neurons lacking PP2A might therefore indicate globally altered actin dynamics (Fig 4). These results will be important leads in order to better define the role of PP2A and actin regulation during dendrite pruning in the future. Since the data presented by us and others [23,24] suggest that loss of PP2A affects actin dynamics and hence possibly both F-actin assembly and disassembly, it is interesting to speculate that the underlying causes for the larval dendrite morphogenesis defects and the pruning defects may be similar. We therefore tentatively place PP2A in a pathway at least partially in parallel to Mical during dendrite pruning (Fig 6).

While our genetic data suggest that PP2A is not involved in the temporal regulation of microtubule disassembly via the Par-1/tau pathway (Fig EV3), the parallel study by the Yu lab [38] found that loss of PP2A leads to a defect in dendritic microtubule orientation. We have previously found that the uniform plus end-in orientation of dendritic microtubules is required for dendrite pruning [14]. It is therefore conceivable that these microtubule-based defects also contribute to the observed dendrite pruning defects. Which of the observed defects in gene expression, microtubule orientation and actin dynamics contributes most to the observed defects remains to be seen. However, the combination of the two studies clearly establishes PP2A as a broad and important regulator of the neuronal cytoskeleton during development.

## Materials and Methods

### Fly strains

All crosses were done at 25°C under standard conditions. For expression in *c4da* neurons, we used *ppk-GAL4* insertions on the second and third chromosomes [41]. MARCM clones were induced with *SOP-FLP* [42] and labeled by tdTomato expression under *nsyb-GAL4<sup>RS7C10</sup>* [43]. Here, the PP2A mutant allele PP2A-29B<sup>GE16781</sup> [26] was recombined with *FRT40A*. Other fly lines were UAS-Mical [44], UAS-MicalΔCH, UAS-MicalΔRedox [27], UAS-Sox14 [39], UAS-tdtomato [17], UAS-*tsr*, UAS-*tsrS3A*, UAS-*tsrS3E* (BL #9235, 9237, 9239) [32], UAS-*lacZ*, UAS-*lifeAct::GFP* (BL 35544), UAS-*dnMts* [45], UAS-PAR-1 [9], UAS-Venus-*kat60L1* [46], tau<sup>KO</sup> [47], *FRT G13*, *tsr<sup>N121</sup>* (BL #9109), *FRT 82B*, *wdb<sup>14</sup>* (BL #53712) [45], UAS-aPKCΔN (BL #51673) UAS-RacN17 (BL #6292), UAS-RhoN19 (BL #7328), and *ena<sup>210</sup>/CyO* (BL #25404). UAS-dsRNA lines were as follows: PP2A-29B (BL #29384), *Wrd* (BL #30512), *Tws* (VDRC# 34340), *chicadee* (VDRC #102759), *moesin* (VDRC #37917). Orco dsRNA (BL #31278) was used as control. UAS-dsRNA lines were used with UAS-dicer2 [48]. For conditional *Tws* and CG4733 CRISPR [49], we used UAS-Cas9P2 (BL #58986). For kinase manipulations, we used UAS-PKA *mc\** and UAS-PKAr\* [50], UAS-LIMK [31], UAS-*abl* [51], and UAS-TOR<sup>TED</sup> [52].

### Cloning and transgenes

*HAPP2A-29B* and *GFP::tsr* were cloned into pUAST attB by standard methods. Transgenes were injected in flies carrying the 86Fb acceptor site [53].

### Dissection, microscopy, and live imaging

For analysis of pruning defects, pupae were dissected out of the pupal case at 18 h APF and analyzed live using a Zeiss LSM 710 confocal microscope. For PP2A-29B genetic interactions, candidate modifiers were crossed to a second chromosome insertion of *ppk-GAL4* combined with UAS-CD8GFP and UAS-dicer2 and UAS-PP2A-29B dsRNA on the third chromosome (BL# 29384). UAS-GFP::*tsr* was expressed under *ppk-GAL4* and imaged live in ether-anaesthetized third-instar larvae or at 6 h APF. All images were analyzed using Fiji [54].

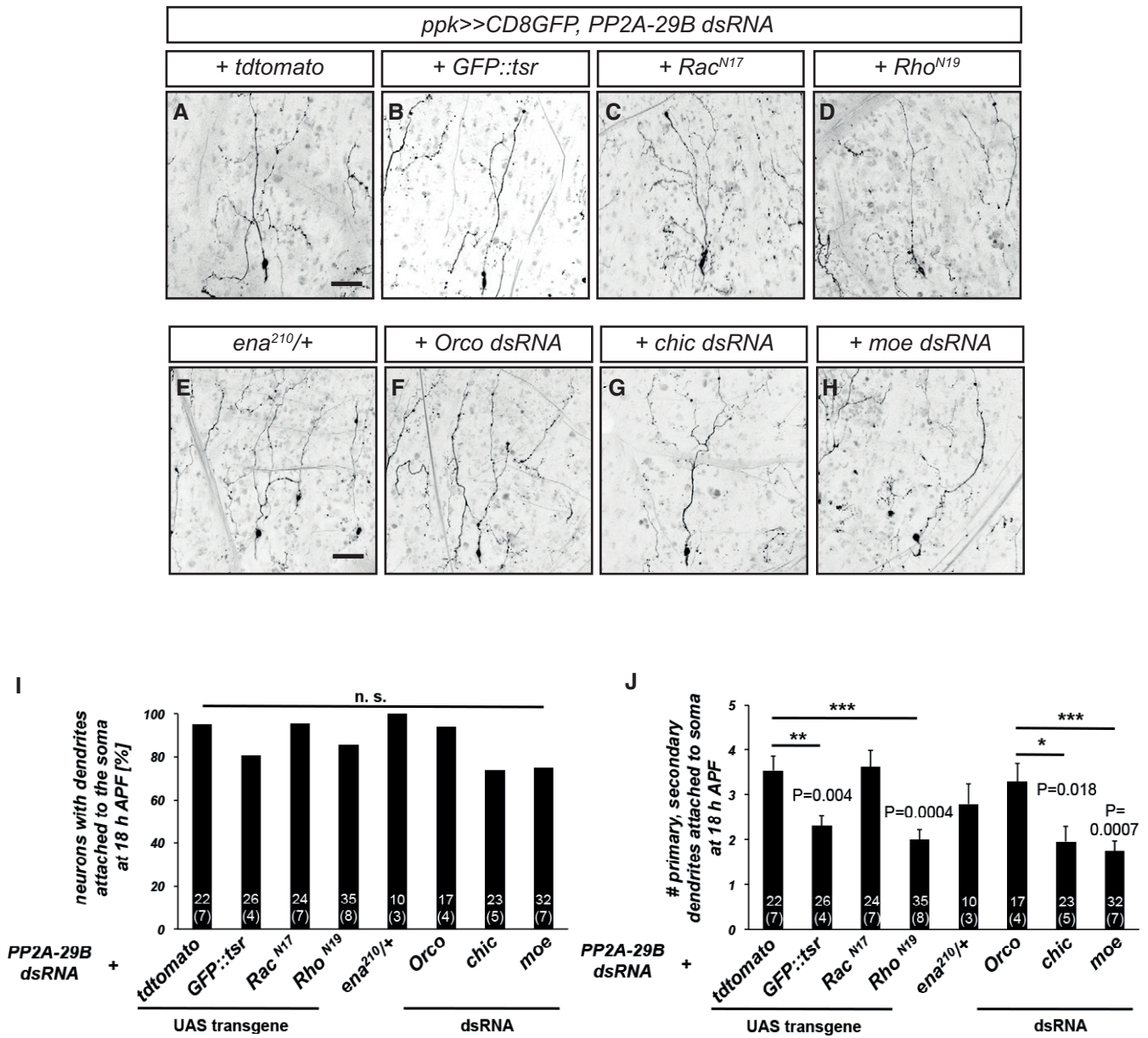


**Figure 5. PP2A interacts with actin regulators during dendrite pruning.**

A–H Genetic interactions between PP2A-29B and actin regulators during dendrite pruning. The indicated manipulations of actin regulators were tested for their ability to suppress pruning defects induced by PP2A-29B dsRNA expression. Suppression tests were performed as in Fig 2. (A) C4da neuron coexpressing PP2A-29B dsRNA and *tdTomato* as suppression control. (B) C4da neuron coexpressing PP2A-29B dsRNA and *GFP::tsr*. (C) C4da neuron coexpressing PP2A-29B dsRNA and *Rac<sup>N17</sup>*. (D) C4da neuron coexpressing PP2A-29B dsRNA and *Rho<sup>N19</sup>*. (E) C4da neuron expressing PP2A-29B dsRNA in *ena<sup>210/+</sup>* background. (F) C4da neuron coexpressing PP2A-29B dsRNA and *Orco* dsRNA as suppression control. (G) C4da neuron coexpressing PP2A-29B dsRNA and *Chicadee* dsRNA. (H) C4da neuron coexpressing PP2A-29B dsRNA and *moesin* dsRNA.

I Penetrance of pruning defects in panels (A–H). n.s., not significant, Fisher’s exact test. Numbers of neurons (animals) for each genotype are given in the figure.

J Severity of pruning defects in panels (A–H) as assessed by number of primary and secondary dendrites attached to soma at 18 h APF. Data are mean ± s.d.,

\**P* < 0.05, \*\**P* < 0.005, \*\*\**P* < 0.0005, Wilcoxon’s test. Numbers of neurons (animals) for each genotype are given in the figure.

Data information: Scale bars in (A and E) are 50 μm.

### Antibodies and immunohistochemistry

Pupal body wall filets were dissected quickly in PBS and fixed in PBS containing 4% formaldehyde for 20 minutes. Chicken anti-GFP antibodies were from Aves labs, respectively. Other antibodies were guinea pig anti-Sox14 [55] and rabbit anti-Mical [40].

### Quantification and statistical analysis

Pruning phenotypes in Figs 1, 2, 4, and 5 were analyzed by determining the fraction of neurons that still had dendrites attached to the soma to reflect the phenotypic penetrance, and these data were analyzed using a two-tailed Fisher’s exact test.

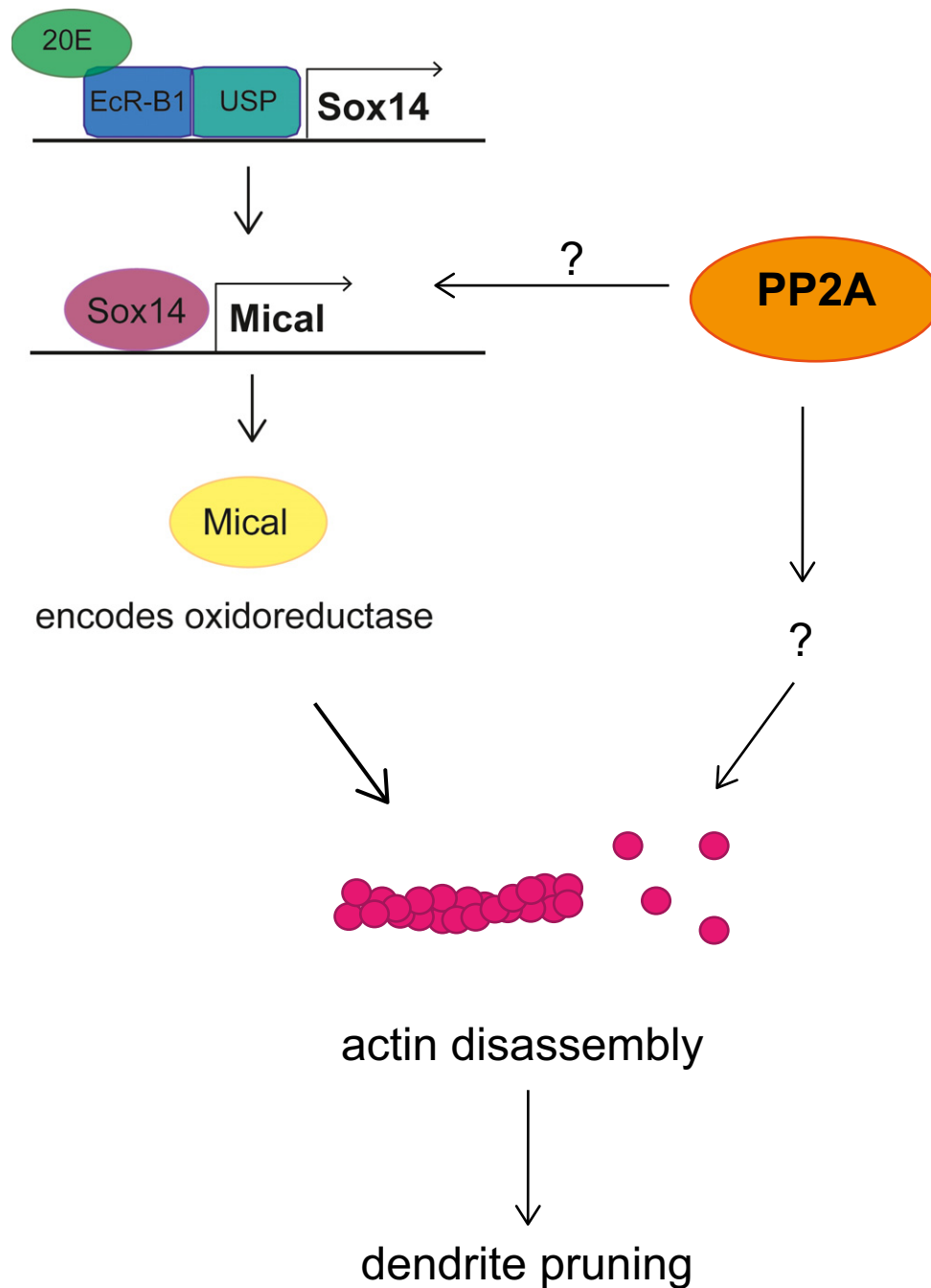


**Figure 6. Hypothetical model for PP2A action during dendrite pruning.**

Our data indicate a two-pronged effect of PP2A on pruning: firstly, PP2A is required for timely expression of Mical via an unknown mechanism. Secondly, PP2A appears to affect actin dynamics in neurons during both the larval and pupal stages.

To assess severity, we also counted the number of primary and secondary branches (i.e., the sum of all primary and secondary dendrites per neuron) still attached to the soma at 18 h APF. These data were analyzed using Wilcoxon's test. In a similar way, we determined the number of neurons with unusual varicosities in Fig 5A–C.

For quantification of immunofluorescence experiments, c4da neuron staining intensities were measured in Fiji and normalized to

c1da neuron staining intensities in the same image. These data were analyzed using Wilcoxon's test.

The number of GFP::tsr punctae was mean  $\pm$  s.d. and analyzed using Wilcoxon's test. For dendritic field coverage analysis, dendritic fields were defined by segment border dendrites (in the anterior/posterior direction), the dorsal midline, and the middle between dorsal and lateroventral c4da neuron dendrites (in the dorsoventral direction). Actual coverage was calculated by

connecting outer dendrite terminals with each other as in Ref. [35]. The covered area was then compared to the maximal dendritic field.

**Expanded View** for this article is available online.

## Acknowledgements

We are grateful to C. Klämbt for continuous support and critical reading of the manuscript. We would like to thank F. Yu for communication of results prior to publication and M. Boutros and F. Port for sharing unpublished reagents. We thank C. Klämbt, T. Stürner, G. Tavosanis, M. Krahn, A. Wodarz, and the Bloomington, Kyoto and VDRC stock centers for reagents and fly stocks, A. Althoff for technical support, and Klämbt and Rumpf lab members for discussions. This work was supported by the DFG excellence cluster Cells in Motion (EXC1003). Neele Wolterhoff is a member of the CRC1348 Integrated Research Training Group.

## Author contributions

NW and SR designed and conceived the project and interpreted the data. NW and SR performed experiments. NW, UG, and SR contributed reagents. SR wrote the manuscript.

## Conflict of interest

The authors declare that they have no conflict of interest.

## References

- Riccomagno MM, Kolodkin AL (2015) Sculpting neural circuits by axon and dendrite pruning. *Annu Rev Cell Dev Biol* 31: 779–805
- Schuldiner O, Yaron A (2015) Mechanisms of developmental neurite pruning. *Cell Mol Life Sci* 72: 101–119
- Kuo CT, Jan LY, Jan YN (2005) Dendrite-specific remodeling of *Drosophila* sensory neurons requires matrix metalloproteases, ubiquitin-proteasome, and ecdysone signaling. *Proc Natl Acad Sci USA* 102: 15230–15235
- Williams DW, Truman JW (2005) Cellular mechanisms of dendrite pruning in *Drosophila*: insights from *in vivo* time-lapse of remodeling dendritic arborizing sensory neurons. *Development* 132: 3631–3642
- Kirilly D, Gu Y, Huang Y, Wu Z, Bashirullah A, Low BC, Kolodkin AL, Wang H, Yu F (2009) A genetic pathway composed of Sox14 and Mical governs severing of dendrites during pruning. *Nat Neurosci* 12: 1497–1505
- Hung R-J, Pak CW, Terman JR (2011) Direct redox regulation of F-actin assembly and disassembly by Mical. *Science* 334: 1710–1713
- Loncle N, Williams DW (2012) An interaction screen identifies headcase as a regulator of large-scale pruning. *J Neurosci* 32: 17086–17096
- Lee H-H, Jan LY, Jan Y-N (2009) *Drosophila* IKK-related kinase Ik2 and Katanin p60-like 1 regulate dendrite pruning of sensory neuron during metamorphosis. *Proc Natl Acad Sci USA* 106: 6363–6368
- Herzmann S, Krumkamp R, Rode S, Kintrup C, Rumpf S (2017) PAR-1 promotes microtubule breakdown during dendrite pruning in *Drosophila*. *EMBO J* 36: 1981–1991
- Kanamori T, Yoshino J, Yasunaga K-I, Dairyo Y, Emoto K (2015) Local endocytosis triggers dendritic thinning and pruning in *Drosophila* sensory neurons. *Nat Commun* 6: 6515
- Zhang H, Wang Y, Wong JJ, Lim KL, Liou YC, Wang H, Yu F (2014) Endocytic pathways downregulate the L1-type cell adhesion molecule Neuroglian to promote dendrite pruning in *Drosophila*. *Dev Cell* 30: 463–478
- Krämer R, Rode S, Rumpf S (2019) Rab11 is required for neurite pruning and developmental membrane protein degradation in *Drosophila* sensory neurons. *Dev Biol* 451: 68–78
- Lin T, Kao HH, Chou CH, Chou CY, Liao YC, Lee HH (2020) Rab11 activation by Ik2 kinase is required for dendrite pruning in *Drosophila* sensory neurons. *PLoS Genet* 16: e1008626
- Herzmann S, Gotzelmann I, Reekers L-F, Rumpf S (2018) Spatial regulation of microtubule disruption during dendrite pruning in *Drosophila*. *Development* 145: dev156950
- Rumpf S, Wolterhoff N, Herzmann S (2019) Functions of microtubule disassembly during neurite pruning. *Trends Cell Biol* 29: 291–297
- Han C, Song Y, Xiao H, Wang D, Franc NC, Jan LY, Jan Y-N (2014) Epidermal cells are the primary phagocytes in the fragmentation and clearance of degenerating dendrites in *Drosophila*. *Neuron* 81: 544–560
- Williams DW, Kondo S, Krzyzanowska A, Hiromi Y, Truman JW (2006) Local caspase activity directs engulfment of dendrites during pruning. *Nat Neurosci* 9: 1234–1236
- Stürner T, Tatarnikova A, Mueller J, Schaffran B, Cuntz H, Zhang Y, Nemethova M, Bogdan S, Small V, Tavosanis G (2019) Transient localization of the Arp2/3 complex initiates neuronal dendrite branching *in vivo*. *Development* 146: dev171397
- Nithianandam V, Chien C-T (2018) Actin blobs prefigure dendrite branching sites. *J Cell Biol* 217: 3731–3746
- Das R, Bhattacharjee S, Patel AA, Harris JM, Bhattacharya S, Letcher JM, Clark SG, Nanda S, Iyer EPR, Ascoli GA et al (2017) Dendritic cytoskeletal architecture is modulated by combinatorial transcriptional regulation in *Drosophila melanogaster*. *Genetics* 207: 1401–1421
- Sontag E, Nunbhakdi-Craig V, Lee G, Bloom GS, Mumby MC (1996) Regulation of the phosphorylation state and microtubule-binding activity of Tau by protein phosphatase 2A. *Neuron* 17: 1201–1217
- Sandí MJ, Marshall CB, Balan M, Coyaud É, Zhou M, Monson DM, Ishiyama N, Chandrakumar AA, La Rose J, Couzens AL et al (2017) MARK3-mediated phosphorylation of ARHGAP23 couples microtubules to the actin cytoskeleton to establish cell polarity. *Sci Signal* 10: ean3286
- Madsen CD, Hooper S, Tozluoglu M, Bruckbauer A, Fletcher G, Erler JT, Bates PA, Thompson B, Sahai E (2015) STRIPAK components determine mode of cancer cell migration and metastasis. *Nat Cell Biol* 17: 68–80
- Yeh PA, Chang CJ (2017) A novel function of twins, B subunit of protein phosphatase 2A, in regulating actin polymerization. *PLoS One* 12: e0186037
- Lee T, Luo L (1999) Mosaic analysis with a repressible cell marker for studies of gene function in neuronal morphogenesis. *Neuron* 22: 451–461
- Krahn MP, Egger-Adam D, Wodarz A (2009) PP2A antagonizes phosphorylation of Bazooka by PAR-1 to control apical-basal polarity in dividing embryonic neuroblasts. *Dev Cell* 16: 901–908
- Riedl J, Crevenna AH, Kessenbrock K, Yu JH, Neukirchen D, Bista M, Bradke F, Jenne D, Holak TA, Werb Z et al (2008) Lifeact: a versatile marker to visualize F-actin. *Nat Methods* 5: 605–607
- Hung R-J, Yazdani U, Yoon J, Wu H, Yang T, Gupta N, Huang Z, van Berkel WJH, Terman JR (2010) Mical links semaphorins to F-actin disassembly. *Nature* 463: 823–827
- Grintsevich EE, Yesilyurt HG, Rich SK, Hung R-J, Terman JR, Reisler E (2016) F-actin dismantling through a redox-driven synergy between Mical and cofilin. *Nat Cell Biol* 18: 876–885
- Arber S, Barbayannis FA, Hanser H, Schneider C, Stanyon CA, Bernard O, Caroni P (1998) Regulation of actin dynamics through phosphorylation of cofilin by LIM-kinase. *Nature* 393: 805–809

31. Yang N, Higuchi O, Ohashi K, Nagata K, Wada A, Kangawa K, Nishida E, Mizuno K (1998) Cofilin phosphorylation by LIM-kinase 1 and its role in Rac-mediated actin reorganization. *Nature* 393: 809–812
32. Niwa R, Nagata-Ohashi K, Takeichi M, Mizuno K, Uemura T (2002) Control of actin reorganization by Slingshot, a family of phosphatases that dephosphorylate ADF/cofilin. *Cell* 108: 233–246
33. Ng J, Luo L (2004) Rho GTPases regulate axon growth through convergent and divergent signaling pathways. *Neuron* 44: 779–793
34. Bamburg JR, Bloom GS (2009) Cytoskeletal pathologies of Alzheimer disease. *Cell Motil Cytoskeleton* 66: 635–649
35. Grueber WB, Jan LY, Jan YN (2002) Tiling of the *Drosophila* epidermis by multidendritic sensory neurons. *Development* 129: 2867–2878
36. Flynn KC, Hellal F, Neukirchen D, Jacob S, Tahirovic S, Dupraz S, Stern S, Garvalov BK, Gurniak C, Shaw AE et al (2012) ADF/cofilin-mediated actin retrograde flow directs neurite formation in the developing brain. *Neuron* 76: 1091–1107
37. Wong JJJ, Li S, Lim EKH, Wang Y, Wang C, Zhang H, Kirilly D, Wu C, Liou Y-C, Wang H et al (2013) A Cullin1-based SCF E3 ubiquitin ligase targets the InR/PI3K/TOR pathway to regulate neuronal pruning. *PLoS Biol* 11: e1001657
38. Rui M, Ng KS, Tang Q, Bu S, Yu F (2020) Protein phosphatase PP2A regulates dendritic microtubule orientation and dendrite pruning in *Drosophila* sensory neurons. *EMBO Rep* 21: e48843
39. Rumpf S, Bagley JA, Thompson-Peer KL, Zhu S, Gorczyca D, Beckstead RB, Jan LY, Jan YN (2014) *Drosophila* Valosin-Containing Protein is required for dendrite pruning through a regulatory role in mRNA metabolism. *Proc Natl Acad Sci USA* 111: 7331–7336
40. Rode S, Ohm H, Anhauser L, Wagner M, Rosing M, Deng X, Sin O, Leidel SA, Storkebaum E, Rentmeister A et al (2018) Differential requirement for translation initiation factor pathways during ecdysone-dependent neuronal remodeling in *Drosophila*. *Cell Rep* 24: 2287–2299.e4
41. Grueber WB, Ye B, Yang C-H, Younger S, Borden K, Jan LY, Jan Y-N (2007) Projections of *Drosophila* multidendritic neurons in the central nervous system: links with peripheral dendrite morphology. *Development* 134: 55–64
42. Matsubara D, Horiuchi S-Y, Shimono K, Usui T, Uemura T (2011) The seven-pass transmembrane cadherin Flamingo controls dendritic self-avoidance via its binding to a LIM domain protein, Espinas, in *Drosophila* sensory neurons. *Genes Dev* 25: 1982–1996
43. Pfeiffer BD, Jenett A, Hammonds AS, Ngo T-TB, Misra S, Murphy C, Scully A, Carlson JW, Wan KH, Laverly TR et al (2008) Tools for neuroanatomy and neurogenetics in *Drosophila*. *Proc Natl Acad Sci USA* 105: 9715–9720
44. Terman JR, Mao T, Pasterkamp RJ, Yu H-H, Kolodkin AL (2002) MICALs, a family of conserved flavoprotein oxidoreductases, function in plexin-mediated axonal repulsion. *Cell* 109: 887–900
45. Hannus M, Feiguin F, Heisenberg CP, Eaton S (2002) Planar cell polarization requires Widerborst, a B' regulatory subunit of protein phosphatase 2A. *Development* 129: 3493–3503
46. Stewart A, Tsubouchi A, Rolls MM, Tracey WD, Sherwood NT (2012) Katanin p60-like1 promotes microtubule growth and terminal dendrite stability in the larval class IV sensory neurons of *Drosophila*. *J Neurosci* 32: 11631–11642
47. Burnouf S, Gronke S, Augustin H, Dols J, Gorsky MK, Werner J, Kerr F, Alic N, Martinez P, Partridge L (2016) Deletion of endogenous Tau proteins is not detrimental in *Drosophila*. *Sci Rep* 6: 23102
48. Dietzl G, Chen D, Schnorrer F, Su K-C, Barinova Y, Fellner M, Gasser B, Kinsey K, Oettel S, Scheiblaue S et al (2007) A genome-wide transgenic RNAi library for conditional gene inactivation in *Drosophila*. *Nature* 448: 151–156
49. Port F, Strein C, Stricker M, Rauscher B, Heigwer F, Zhou J, Beyersdorffer C, Frei J, Hess A, Kern K et al (2020) A large-scale resource for tissue-specific CRISPR mutagenesis in *Drosophila*. *Elife* 9: e53865
50. Li W, Ohlmeyer JT, Lane ME, Kalderon D (1995) Function of protein kinase A in hedgehog signal transduction and *Drosophila* imaginal disc development. *Cell* 80: 553–562
51. Fogerty FJ, Juang JL, Petersen J, Clark MJ, Hoffmann FM, Mosher DF (1999) Dominant effects of the bcr-abl oncogene on *Drosophila* morphogenesis. *Oncogene* 18: 219–232
52. Hennig KM, Neufeld TP (2002) Inhibition of cellular growth and proliferation by dTOR overexpression in *Drosophila*. *Genesis* 34: 107–110
53. Bischof J, Maeda RK, Hediger M, Karch F, Basler K (2007) An optimized transgenesis system for *Drosophila* using germ-line-specific phiC31 integrases. *Proc Natl Acad Sci USA* 104: 3312–3317
54. Schindelin J, Arganda-Carreras I, Frise E, Kaynig V, Longair M, Pietzsch T, Preibisch S, Rueden C, Saalfeld S, Schmid B et al (2012) Fiji: an open-source platform for biological-image analysis. *Nat Methods* 9: 676–682
55. Ritter AR, Beckstead RB (2010) Sox14 is required for transcriptional and developmental responses to 20-hydroxyecdysone at the onset of *Drosophila* metamorphosis. *Dev Dyn* 239: 2685–2694



**License:** This is an open access article under the terms of the Creative Commons Attribution 4.0 License, which permits use, distribution and reproduction in any medium, provided the original work is properly cited.